A Draft Map of the Human Ovarian Proteome for Tissue Engineering and Clinical Applications

Emna Ouni‡, Didier Vertommen§, Maria Costanza Chiti‡, Marie-Madeleine Dolmans‡¶, and Christiani A. Amorim‡‖

Fertility preservation research in women today is increasingly taking advantage of bioengineering techniques to develop new biomimetic materials and solutions to safeguard ovarian cell function and microenvironment *in vitro* and *in vivo*. However, available data on the human ovary are limited and fundamental differences between animal models and humans are hampering researchers in their quest for more extensive knowledge of human ovarian physiology and key reproductive proteins that need to be preserved. We therefore turned to multi-dimensional label-free mass spectrometry to analyze human ovarian cortex, as it is a high-throughput and conclusive technique providing information on the proteomic composition of complex tissues like the ovary. In-depth proteomic profiling through two-dimensional liquid chromatography-mass spectrometry, Western blotting, histological and immunohistochemical analyses, and data mining helped us to confidently identify 1508 proteins. Moreover, our method allowed us to chart the most complete representation so far of the ovarian matrisome, defined as the ensemble of extracellular matrix proteins and associated factors, including more than 80 proteins. In conclusion, this study will provide a better understanding of ovarian proteomics, with a detailed characterization of the ovarian follicle microenvironment, in order to enable bioengineers to create biomimetic scaffolds for transplantation and three-dimensional *in vitro* culture. By publishing our proteomic data, we also hope to contribute to accelerating biomedical research into ovarian health and disease in general. ***Molecular & Cellular Proteomics 18: 10.1074/mcp.RA117.000469, S159–S173, 2019.***

The World Health Organization has ranked infertility in women as the fifth highest serious global disability (1). Based on this critical assessment, several strategies have been developed to preserve and even restore fertility in women.

Although the human ovary is relatively well understood in terms of secretory patterns of ovarian hormones and the pathogenesis of ovarian diseases, little is known about the molecular composition and regulation of the microenvironment that directs the development and function of ovarian follicles, the functional units that mainly reside in the ovarian cortex and play an important role in oogenesis and gonadal hormone secretion. A few studies have focused on mRNA expression to provide a complete characterization of gene expression in the ovary. However, study of gene expression at the mRNA level yields no information about post-transcriptional modifications (2). Moreover, even abundant mRNA transcripts may be translated inefficiently or degrade rapidly, resulting in lower than expected levels of protein expression (3).

On the other hand, by focusing on final gene products, a proteomic approach has the advantage of investigating complex biological events and diseases, providing more conclusive information.

For several years now, ovarian proteomic studies have concentrated on characterizing follicular fluid composition in human preovulatory follicles (4–5), emphasizing the functional selectivity of the basement membrane toward plasma proteins (6). Efforts have also been made to identify ovary-related transcription in different species to explore the complex functions of the ovary in an integrated manner. This is necessary because of obvious difficulties in obtaining human ovaries, as well as the feasibility of conducting experimental research in humans because of ethical and logistical constraints. He *et al.* (2015). described ovarian proteomics in rhesus monkeys through identification of 4325 proteins to provide a basis for future studies of human reproductive disorders using this

From the ‡Pôle de Recherche en Gynécologie, Institut de Recherche Expérimentale et Clinique, Université Catholique de Louvain, Brussels, Belgium; §de Duve Institute, Université Catholique de Louvain, Brussels, Belgium; ¶Gynecology Department, Cliniques Universitaires Saint-Luc, Brussels, Belgium

Received November 15, 2017, and in revised form, February 15, 2018
Published, MCP Papers in Press, February 23, 2018, DOI 10.1074/mcp.RA117.000469
Author contributions: E.O. and C.A.A. designed research; E.O. performed research; E.O. and D.V. analyzed data; E.O. wrote the paper; D.V. contributed new reagents/analytic tools; M.C.C. participated in experimental procedures; M.-M.D. controlled the clinical aspect of the study and revised critically the manuscript; C.A.A. helped in result interpretation and revised critically the manuscript.

animal as a model (7). To our knowledge, the only proteomic analysis of human ovaries performed to date was conducted by Wang *et al.* (2005) (8). The study identified 138 proteins by two-dimensional (2D) electrophoresis and MALDI-TOF mass spectrometry, but without differentiation of ovarian extracellular matrix (ECM)[1] proteins, despite the ECM's important role in defining the follicular environment and orchestrating cellular organization and function. Indeed, the only aspect of the ovarian ECM to have been investigated so far is the basement follicular membrane, and this was done through immunohistochemical tests, which only offer a limited characterization restricted by the type and number of antibodies used (9–10).

The goal of this study was therefore to provide a draft map of functional proteins identified in human ovarian cortex and complement available ovarian ECM data. By using 2D liquid chromatography-mass spectrometry (2D-LC/MS) and ensuring adequate sample preparation, we aimed to shed light on potential key intra- and extracellular proteins in reproduction, to form a basis for comparative studies between normal and pathological ovaries and open the door to improved bioengineering techniques for creation of better biomimetic scaffolds.

EXPERIMENTAL PROCEDURES

Experimental Design and Statistical Rationale—This study involved six 2D-LC/MS experiments using human ovarian cortex from three patients undergoing laparoscopic surgery for benign gynecologic disease. Fresh and cryopreserved samples derived from the same biopsy were analyzed. Each biopsy from each of the patients was initially divided into two fragments; one was immediately analyzed (fresh tissue) and the other was frozen and thawed before analysis (frozen), totaling six experiments. Because the ovarian biopsies were obtained from patients with healthy ovaries, only a small portion of their ovarian tissue was taken ($\leq$9 mm^2) so as not to impact their ovarian activity. For this reason, we could not carry out technical replicates. Moreover, the scarcity of fresh human ovarian biopsies limited the number of samples available for analysis.

To provide a descriptive draft map of ovarian tissue, a threshold was maintained to select the most confidently detected proteins. This threshold included proteins with a Sequest HT score $\geq$10 in any of the 6 samples for gene ontology and pathway analyses. Each protein score was calculated by the Proteome Discoverer application as follows: *protein score = (sum of all cross-correlation factors of 0.8 or above) + (peptide charge × peptide relevance factor),* the default value for the peptide relevance factor being 0.4.

To establish a draft map of the ovarian matrisome, only proteins with a score $\geq$10 in any of the 6 samples and identified by at least two unique peptides in three or more samples were considered.

Fresh and frozen sample compositions were compared based on spectral counts for each detected matrisome protein. A formal quantitative approach was first attempted to carry out comparisons through a paired *t* test. However, a number of issues emerged with this type of test, making it hard to draw any conclusions: (1) small sample size because of limited availability of patients; (2) inability to justify the normality of data, possibly warranting use of non-parametric tests; and (3) need for multiple testing, requiring adequate adjustment (inflation) of *p* values. The first preliminary results pointed to only a few significant ($p < 0.05$) outcomes (proteins) before adjustment, whereas after adjustment (Benjamini-Hochberg), none of the proteins remained significant. It would therefore be naive to conclude that this somehow proves equivalence. In view of the small sample size and the fact that multiplicity corrections typically suppress detection to avoid false positives, we did not feel that this quantitative argument was sound enough to yield any conclusions. A qualitative, more descriptive approach was therefore pursued, considering the importance of comparing protein content and immunohistochemistry results between fresh and frozen tissues.

Collection of Ovarian Tissue and Biopsy Processing—Use of human ovarian cortex was approved by the Institutional Review Board of the Université Catholique de Louvain on November 28, 2016 (IRB reference 2012/23MAR/125, registration number B403201213872). Ovarian biopsies were taken from 3 women (30, 49, and 59 years of age) after obtaining their informed consent. All patients were undergoing laparoscopic surgery for benign gynecologic disease not related to the ovaries (supplemental Table S2). Biopsies were immediately transported on ice to the laboratory in minimal essential medium (MEM)-Glutamax (Gibco, Invitrogen, Merelbeeke, Belgium) and rigorously washed in Dulbecco's phosphate-buffered saline (DPBS) (Gibco) to remove blood remains.

The cortical area of the ovary was selected for analysis, as it is the reservoir of most of the follicle population and would therefore provide the greatest insights into the follicular microenvironment and regulatory factors. Hence, the medullary part of the biopsy was removed, and the cortex was cut into small fragments. A small piece of each biopsy was fixed in formalin and the remaining fragments were either immediately digested or cryopreserved.

Tissue Preparation for Fresh Ovarian Cortex—For extraction of intra- and extracellular proteins, including ECM proteins, we applied a modified version of our isolation protocol for human preantral follicles (11). Ovarian cortical fragments were first subjected to mechanical digestion using a tissue chopper (McIlwain Tissue Chopper; Mickle Laboratory, Guilford, UK), before being, incubated with 0.28 Wünsch units/ml Liberase DH (Roche Diagnostics, GmbH, Mannheim, Germany) diluted in 5 ml DPBS in a water bath at 37 °C with mild agitation. After 30 min, the suspension was centrifuged at 260 × *g* for 15 min at 4 °C, the supernatant was collected, and the action of Liberase was inhibited with 20 mM EDTA (Sigma, Bornem, Belgium). The sample was then stored at −80 °C until MS analysis.

Tissue Preparation for Frozen Ovarian Cortex—Freezing of ovarian cortex was performed using our routine protocol (12). Briefly, the ovarian fragments were suspended in a cryoprotective solution consisting of MEM-Glutamax (Gibco) supplemented with 4 mg/ml human serum albumin (HSA, Bornem, Belgium) at 4 °C, and transferred to 2 ml cryovials (Simport, Quebec City, Canada) containing 0.8 ml cryoprotective solution. The cryovials were cooled in a programmable freezer (Freezer Control CL-8800i, CryoLogic, Victoria, Australia) us-

[1] The abbreviations used are: ECM, extracellular matrix; 2D-LC/MS, two-dimensional liquid chromatography mass spectrometry; bFGF, basic fibroblast growth factor; BMP-2, bone morphogenetic protein 2; CGMP-PKG, cyclic GMP-protein kinase G; DAB, 3,3′-diaminobenzidine; EGF, epithelial growth factor; FDR, false discovery rate; GAPDH, glyceraldehyde-3-phosphate dehydrogenase; HILIC, hydrophilic interaction liquid chromatography; HSA, human serum albumin; HSPG2, perlecan; IGF, insulin-like growth factor; IGFALS, insulin-like growth factor-binding protein acid-labile subunit; MEM, minimal essential medium; MMP, matrix metalloproteinase; OGN, mimecan; ORA, overrepresentation enrichment analysis; PARS, platelet-associated regulatory system; PCNA, proliferating cell nuclear antigen; PEDF, pigment epithelium-derived factor; PI3K-Akt, phosphoinositide 3-kinase serine/threonine kinase Akt; PSM, peptide spectrum match; RAS, renin-angiotensin system; SLRP, small leucine-rich proteoglycan; TBS, tris-buffered saline; VEGF, vascular endothelial growth factor; αSMA, alpha-smooth muscle actin.

ing the following program: (1) cooled from 0 °C to −8 °C at −2 °C/min; (2) seeded manually; (3) cooled to −40 °C at −0.3 °C; and (4) cooled to −140 °C at −30 °C/min before being transferred to liquid nitrogen (−196 °C) for storage. After 24 h in liquid nitrogen, the cryovials were exposed to room temperature for 2 min and immersed in a water bath at 37 °C until the ice completely melted. To remove the cryoprotective solution, the ovarian cortical pieces were immediately transferred from the cryovials to plastic Petri dishes containing MEM, where they were washed three times (5 min per bath). A fragment from each sample was then fixed in formalin and the rest was digested and stored at −80 °C, as described above for fresh tissue.

Sample Preparation for Mass Spectrometry Analysis—Total protein content was quantified by the Bradford assay. Three hundred μg of proteins was reduced using 5 mM DTT and incubated at 56 °C for 20 min. After cooling to room temperature, cysteines were alkylated by addition of 30 mM chloroacetamide for 25 min.

Proteins were then precipitated by adding TCA to a final concentration of 10% [w/v]. After centrifugation at 14000 rpm for 5 min at 4 °C, the pellet was resuspended in 100 mM ammonium bicarbonate (pH 8.0) and 0.5 M urea, with continuous vortexing and sonication. Protein digestion was performed using trypsin at an enzyme/substrate ratio of 1:100 [wt/wt] overnight at 30 °C (Promega, Madison, WI). The reaction was halted by adding TFA to a final concentration of 0.1% [v/v] and the sample was stored at −20 °C.

Label-free Differential 2D-LC/MS—Tryptic digests were first desalted and concentrated on HyperSep C18 cartridges (50 mg/ml, Thermo Scientific, San Jose, CA) according to the manufacturer's instructions. Peptides were then loaded onto a hydrophilic interaction liquid chromatography (HILIC) TSKgel amide-80 column (4.6 mm by 25 cm; Tosoh Bioscience, Stuttgart, Germany) equilibrated with solvent B (98% ACN [v/v], 0.1% TFA [v/v] in water) and connected to an Agilent 1100 HPLC system. The peptides were separated using a 70-min elution gradient that consisted of 5% to 45% solvent A (2% ACN [v/v], 0.1% TFA [v/v] in water) at a flow rate of 500 μl/min. Absorbance was monitored at 214 nm to ensure that all samples contained similar amounts of material. Fractions were collected at 2-min intervals (starting at 30-min elution, 20 in total) and dried using a Speedvac. Peptides were resuspended in 10 μl of solvent C (3.5% ACN [v/v], 0.1% TFA [v/v] in water) and analyzed by LC-MS/MS. The LC-MS/MS system consisted of an LTQ XL IT mass spectrometer (Thermo Scientific) equipped with a microflow ESI source. Samples (6.5 μl) were injected and desalted on a peptide trap (C18 Pepmap 0.30 × 5 mm, ThermoScientific) equilibrated with solvent C (3.5% ACN [v/v], 0.1% TFA [v/v] in water) at a flow rate of 30 μl/min. After valve switching, peptides were eluted in backflush mode from the trap onto the analytical column (BioBasic C18 0.18 × 150 mm, ThermoScientific) equilibrated in solvent D (5% ACN [v/v], 0.05% formic acid [v/v] in water) and separated using a 70-min gradient from 0% to 70% solvent E (80% ACN [v/v], 0.05% formic acid [v/v] in water) at a flow rate of 1.5 μl/min. The MS scan routine was set to analyze, by MS/MS, the five most intense ions of each full MS scan, with dynamic exclusion enabled to ensure detection of co-eluting peptides.

Protein Identification and Quantitation—Protein identification was performed with Sequest HT. More specifically, peak lists were generated by Extract-MSn (Thermo Scientific) within Proteome Discoverer 1.4.2. From raw files, MS/MS spectra were exported using the following settings: peptide mass range 350–5000 Da, minimal total ion intensity 500. The resulting peak lists were searched using Sequest HT against a human protein database obtained from UniProt (March 1, 2014, 87,489 entries). The following parameters were applied: trypsin was selected with proteolytic cleavage only after arginine and lysine; the number of internal cleavage sites was set to 1; mass tolerance for precursors and fragment ions was 1.0 Da; and considered dynamic modifications were +15.99 Da for oxidized methionine and +57.00 for carbamidomethyl cysteine. Peptide matches were filtered using the q-value and posterior error probability calculated by the Percolator algorithm, ensuring an estimated false discovery rate (FDR) below 5%. Filtered Sequest HT output files for each peptide were grouped according to the protein from which they were derived, and their individual peptide spectrum match (PSM) score was taken as an indicator of protein abundance. No normalization procedure was required because sampling rates (*mean PSM ÷ number of detected proteins*) were similar between all samples (17 ± 0.57 in fresh samples and 16 ± 0.44 in frozen samples). These MS proteomic data were deposited in the ProteomeXchange Consortium database via the PRIDE partner repository with the data set identifier PXD008183.

Bioinformatics—Gene ontology (biological process and cellular component) analysis of the ensemble of detected proteins was performed through WebGestalt (http://www.WebGestalt.org) and DAVID (https://david.ncifcrf.gov) online databases. Pathway analysis was conducted via the KEGG pathway (http://www.genome.jp/kegg/pathway.html). Identification of matrisome proteins was achieved by comparison against matrisome atlas proteins (13). JMP® 12.2.0 was used to generate qualitative analysis graphs to compare fresh and frozen samples.

Histological and Immunohistochemical Analyses—Histological analysis was performed on fresh and frozen-thawed samples of ovarian cortex. After fixation, the ovarian fragments were dehydrated, embedded in paraffin and serially sectioned (5 μm-thick sections). Every fourth slide was stained with hematoxylin-eosin (Merck, Darmstadt, Germany) for histological evaluation; the other slides (Superfrost® Plus slides, Menzel-Glaser, Braunschweig, Germany) were kept for immunostaining.

Paraffin sections were deparaffinized with Histosafe (Yvsolab SA, Beerse, Belgium) and rehydrated in alcohol series. After blocking endogenous peroxidase activity with 3% H_2O_2 [v/v], epitope unmasking was performed with use of citrate buffer (0.01 M) at 98 °C for 75 min in a water bath or Tris-EDTA-Tween buffer (Tris 10 mM, EDTA 1 mM pH 9.0, Tween 20) at 96 °C for 20 min. Slides were incubated for 30 min with 10% goat serum and 1% BSA to block nonspecific binding sites and then analyzed using primary antibodies to proliferating cell nuclear antigen (PCNA) (1/4000 dilution, Dako, Glostrup, Denmark), desmin (1/50 dilution, Dako), alpha-smooth muscle actin (αSMA) (1/100 dilution, Dako), β-catenin (1/15000 dilution, BD Biosciences, San Diego, USA), emilin-1 (1/50 dilution, Sigma), fibrillin-1 (1/100 dilution, Sigma), collagen IV (1/25 dilution, Dako) and VI (1/100 dilution, Acris, Tokyo, Japan).

Immunohistochemical staining was carried out using 3,3′-diaminobenzidine (DAB) horseradish peroxidase chromogen-based system (EnVision™+, Dako) and hematoxylin as a counterstain. Slides were then mounted with DPX mounting medium (Sigma). Negative control samples were obtained by omission of the primary antibody, whereas placenta was used as a positive control for collagen VI, endometrium as a positive control for PCNA, desmin, αSMA, β-catenin and fibrillin-1, and uterine myoma tissue as a positive control for emilin-1 and collagen IV. Glycosaminoglycans were identified by alcian blue staining at pH 2.5 (Bio-Optica, Milan, Italy) to label carboxylated and sulfated proteoglycans (14). Images were taken with a Nikon Eclipse Ci microscope equipped with a Leica DFC450 camera interfaced to Leica Application Suite V4.5 software.

Western Blotting—Proteins (25 μg) in each sample were precipitated using the methanol:chloroform method, then boiled in 2X Laemmli buffer and loaded onto polyacrylamide gels. Following SDS-PAGE, the proteins were transferred onto PVDF membranes, which were then blocked in Tris-buffered saline (TBS) containing 0.1% [v/v] Tween and 3% [w/v] BSA. Membranes were incubated overnight at

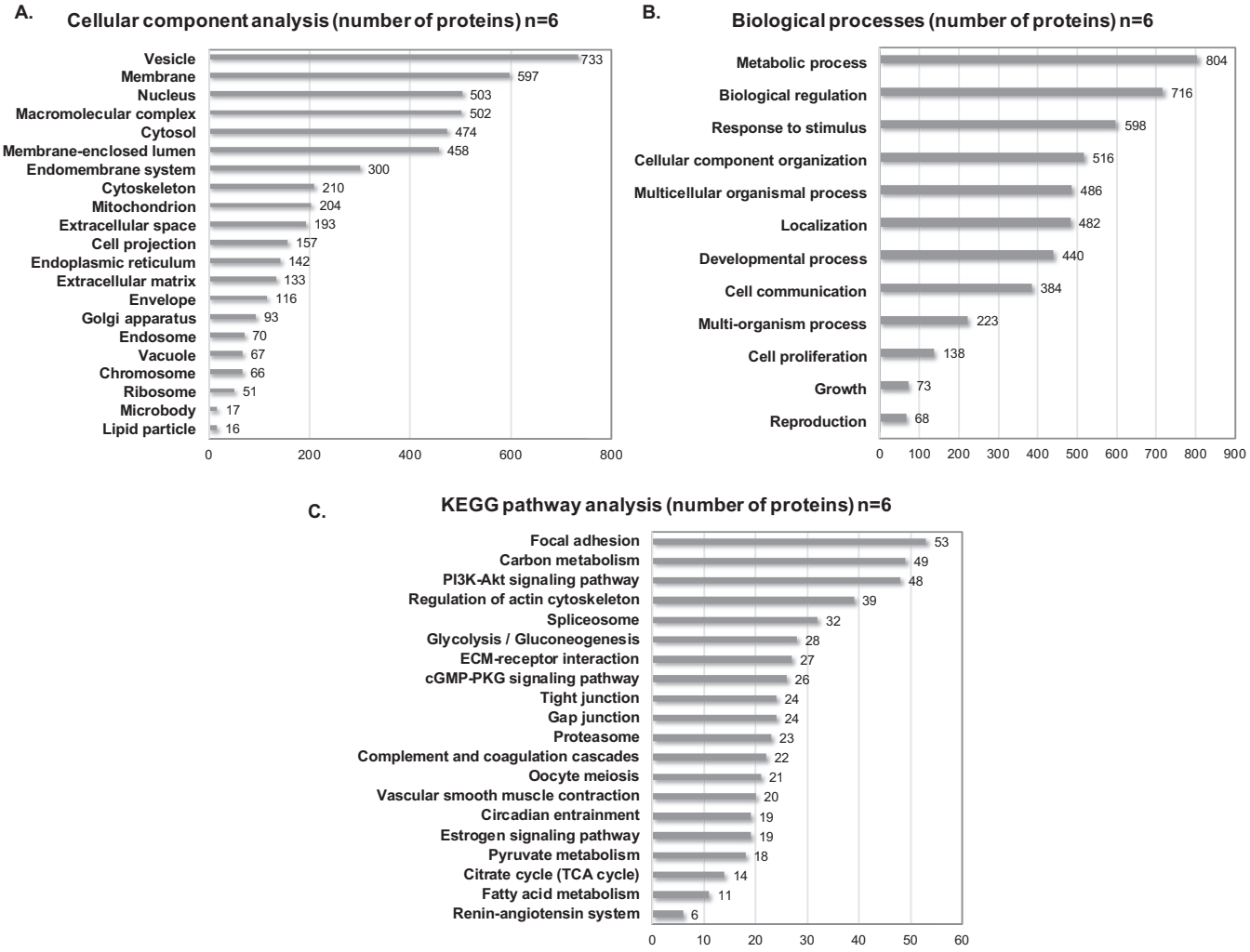

FIG. 1. **Gene ontology and pathway analysis of the ovarian proteome.** *A*, Cellular component analysis. *B*, Biological process analysis. Enriched biological processes and protein localization were achieved using WebGestalt database. *C*, KEGG pathway analysis. Proteins were identified based on conversion of their UniProt accession ID to Entrez Gene.

4 °C with primary antibodies against mimecan (OGN, 1/4000 dilution, Invitrogen, CA, USA) and insulin-like growth factor-binding protein complex acid labile subunit (IGFALS, 1/1000 dilution, OriGene, Rockville, USA), diluted in blocking buffer, then washed extensively in TBS containing 0.1% [v/v] Tween before and after incubation for 1 h with HRP-conjugated secondary antibodies (1/20,000 dilution). Glyceraldehyde-3-phosphate dehydrogenase (GAPDH, 1/10,000 dilution, Merck) was used as a loading control. Immunodetection was achieved with ECL Classico substrate (Merck).

RESULTS

Total Ovarian Proteome Analysis—A total of 5,253 proteins were detected with an FDR <5%, out of which 1508 unique proteins were confidently identified based on a score ≥10. These 1508 proteins were kept for further bioinformatic analysis.

Functional Classification of the Ovarian Proteome and Pathway Analysis—To obtain an extended evaluation of the pool of proteins identified within our samples, we conducted cellular component, biological process and KEGG pathway analyses online using WebGestalt (http://WebGestalt.org) on all detected proteins within the threshold, after converting their UniProt accessions into Entrez Gene and removing duplicates. The following settings were selected to carry out the functional classification: genome protein-coding as a reference set for enrichment analysis, and overrepresentation enrichment analysis (ORA) as a method of reference. We thus obtained a better understanding of the gene ontology of detected proteins within our samples (Fig. 1).

Cellular component analysis revealed, at a glance, the localization of proteins detected by MS and their distribution among cellular compartments (Fig. 1*A*). It is worth mentioning that whereas membrane proteins represented most of detected proteins, it was also possible to extract proteins from different cellular compartments. Indeed, our protein extraction method enabled us to extract and detect, with a high degree of confidence, extracellular as well as intracellular proteins, transmembrane proteins and cell receptors, such as mem-

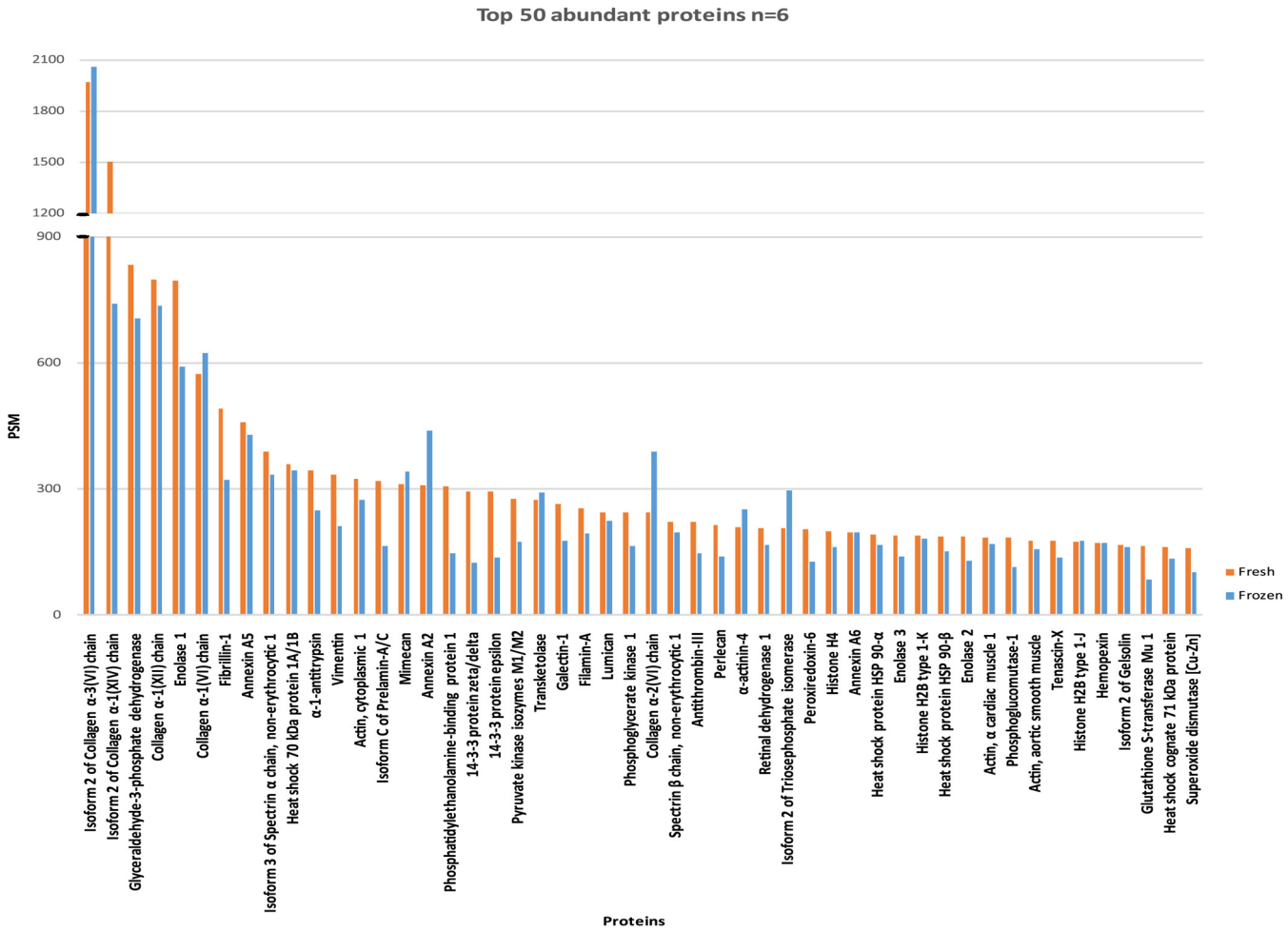

FIG. 2. **TOP 50 most abundant proteins.** After retrieval of the top contaminating plasma proteins from the proteome data set, the most abundant proteins in all samples were classified based on their PSM.

brane-associated progesterone receptor component 1, ryanodine receptor 1 and prolow-density lipoprotein receptor-related protein 1.

Biological process analysis showed many detected proteins to be implicated in metabolic processes, growth, proliferation and communication (Fig. 1*B*). Despite limited available information on ovarian proteomics, 68 proteins were confidently assessed as being involved in reproduction, whereas others were responsive to endogenous and exogenous stimulation, including photosensitive and mechanosensitive proteins.

Relevant biological processes related to reproduction were further investigated through pathway analysis using the KEGG database (Fig. 1*C*), which highlights proteins involved in the phosphoinositide 3-kinase serine/threonine kinase Akt (PI3K-Akt) signaling pathway and oocyte meiosis pathway. Among our proteomic data, we also detected other pathways linked to ovarian activity, such as cyclic GMP-protein kinase G (cGMP/PKG), gap junctions, and estrogen signaling (supplemental Data S1*A*).

Different mechano-regulating pathways chiefly related to smooth muscle contraction and relaxation, like the actin cytoskeleton organization pathway, were also identified. Moreover, because cells function in mutual interaction with the surrounding ECM for ECM regulation, cellular adhesion and activity modulation, we detected ECM-interaction receptors and focal adhesion proteins. Interaction between the ECM and ovarian cells is also governed by matrix metalloproteinases (MMPs), which were encountered, but with a very low PSM and score, reflecting their small proportion compared with other proteins found in our samples. Nevertheless, some ECM degradation proteases were clearly discernible, namely cathepsin G, cathepsin D and plasmin.

Top 50 Detected Proteins—High expression of some proteins in the ovary suggested that they may play specific roles in the maintenance of normal ovarian function (Fig. 2). The 50 most abundant proteins observed in our fresh ($n = 3$) and frozen ($n = 3$) samples were pooled and ranked based on the number of PSMs after retrieval of hemoglobin subunits and top plasma-contaminating proteins: serum albumin, sero-

transferrin, ceruloplasmin, transthyretin, immunoglobulin, complement factors and apolipoprotein A-I (inspired by commercial kits available for plasma protein retrieval from analyzable samples). Around 76% of ranked proteins were recorded among the 50 most commonly found proteins in each individual sample. Collagens, as expected, were the most abundant proteins, mainly collagen VI, followed by cytoskeleton organization proteins (vimentin, α-filamin, actin, actinin) and ECM (annexins, fibrillin-1, galectin, lumican) and cellular regulators (GAPDH, transketolase, 14-3-3 protein zeta/delta) from different cellular compartments. Certain proteoglycans were also widely detected, such as mimecan and perlecan.

Ovarian ECM Proteome Map—Although gene ontology can offer us a preliminary understanding of the cellular compartments, functions and biological processes of proteins, it has clear limitations with respect to ECM protein differentiation and classification, which is why we needed to clearly establish which proteins should be considered part of the ECM. To this end, all proteins detected by MS were compared against the Matrisome Project data (13) to identify all ECM proteins within our samples. Hence, we were able to provide an extended definition of the ovarian ECM, including not only all structural ECM components, but also proteins able to regulate and remodel the ECM. We subsequently categorized our proteins following Naba *et al.* 's (2016) classification (13):

1 Core matrisome proteins: ECM glycoproteins, collagens and proteoglycans.

2 ECM-associated proteins.

- ECM-affiliated proteins: proteins showing biochemical and architectural analogy with ECM proteins or known to be associated.
- ECM regulators: proteins responsible for ECM turnover.
- Secreted factors interacting with core ECM proteins.

The ensemble above forms the matrisome (Fig. 3). Subsequently, only matrisome proteins that were confidently detected based on score and number of unique peptides were retained and their distribution among samples was evaluated and compared between tests, using their PSM values as an estimate of protein abundance. This approach allowed us to constitute the ovarian matrisome draft map consisting of: (1) the core matrisome, including 28 glycoproteins, 11 subtypes of collagen and 7 proteoglycans, representing 15%, 49% and 7% of the total matrisome proteins respectively (Fig. 3 and 4); and (2) matrisome-associated proteins, including 12 ECM-affiliated proteins, 23 ECM regulators and 4 secreted factors, representing around 18%, 10%, and 1% of the total matrisome proteins respectively. This percentage calculation was based on the sum of PSM means of all proteins within the same category (*e.g.* collagens), divided by the sum of PSM means of all matrisome proteins (Fig. 3). Thus, the ECM of human ovarian cortex comprises 85 matrisome proteins in total: 46 core matrisome proteins and 39 matrisome associated-proteins.

As expected, secreted factors and ECM modification enzymes were less abundant than structural proteins and, consequently, less well represented in our data set (Fig. 3).

Comparison Between Fresh and Frozen-Thawed Ovarian Cortex Proteomic Data—In order to evaluate the ability of cryopreserved tissue to reflect fresh tissue proteomic composition, we compared proteomic data from fresh and cryopreserved samples. A comparison of total proteins within each group showed similar variability between fresh and frozen samples (Fig. 5*A*) and, interestingly, an overlap of more than 70% in detected proteins between the two sample types (Fig. 5*B*). Considering only matrisome proteins, analysis of PSM means revealed no clear difference between fresh and frozen-thawed samples among highly abundant proteins. However, the curve showed some differences among less abundant proteins, which are very difficult to detect by MS in complex samples such as ours (Fig. 6).

Histological and Immunohistochemical Analyses—To assess the localization and distribution of detected proteins of interest by MS, 8 proteins from different cellular components with relevant functions in ovarian tissue were analyzed. Fresh and frozen-thawed samples collected from all patients were evaluated and compared by immunohistochemical staining (Fig. 7). It is important to stress that no visible differences between fresh and frozen-thawed tissue samples were observed in any of the selected proteins.

First, to confirm MS data on the dominant type of collagen in ovarian cortex, collagen VI was stained and compared with collagen IV, because it is the most widely characterized collagen type in the ovary (10-15-17). Positive staining for collagen IV was predominantly found in the follicular basement membrane, whereas collagen VI was detected throughout the interstitial ECM, and often close to the basement membrane. Collagen VI has different roles in tissues where it is expressed, ranging from mechanical roles, which are typical of collagen components of the ECM, to more specific cytoprotective functions, counteracting apoptosis and oxidative damage and regulating cell autophagy and differentiation (18).

Mechanical tissue features related to ovarian cyclic evolvement were evaluated using desmin and αSMA as markers of muscle contraction. Although ovarian cortex was highly immunopositive for desmin, it contained lower levels of αSMA, which was mainly present around blood vessels in all analyzed samples.

ECM proteins emilin-1 and fibrillin-1 were investigated as elasticity markers (19–20). Immunostaining results showed broad distribution of both glycoproteins within ovarian cortex in all patient samples with similar localizations, emphasizing the close relationship between structural and regulatory properties of emilin-1 and fibrillin-1 in connective tissue. Emilin-1 is usually distributed in tissues where resilience and elastic recoil are prominent, is known to interact with integrins, and

Core matrisome

PSM
Low High

Glycoproteins

ENTREZ GENE Accession	Protein name	P1 fresh	P1 frozen	P2 fresh	P2 frozen	P3 fresh	P3 frozen	PSM mean
1805	Dermatopontin (DPT)	9	10	17	21	15	12	14
10516	Fibulin 5 (FBLN5)	33	33	18	14	24	21	24
2200	Fibrillin 1 (FBN1)	321	175	214	281	490	321	300
2243	Fibrinogen alpha chain (FGA)	41	25	12	11	19	14	20
2244	Fibrinogen beta chain (FGB)	90	48	67	68	73	38	64
2266	Fibrinogen gamma chain (FGG)	63	65	47	50	55	25	51
3483	Insulin-like growth factor-binding protein acid labile subunit (IGFALS)			7	3	7		6
3908	Laminin subunit alpha 2 (LAMA2)	3	2	1	5	9	4	4
3910	Laminin subunit alpha 4 (LAMA4)	11	7	1	1	2	2	4
3911	Laminin subunit alpha 5 (LAMA5)	115	78	12	26	4	4	40
3912	Laminin subunit beta 1 (LAMB1)	22	15	4	3	2	3	8
3913	Laminin subunit beta 2 (LAMB2)	117	83	32	47	19	20	53
3915	Laminin subunit gamma 1 (LAMC1)	98	78	33	48	14	14	48
4237	Microfibrillar-associated protein 2 (MFAP2)	10	7	11	11	11	17	11
4239	Microfibrillar-associated protein 4 (MFAP4)	35	29	100	102	25	31	54
4811	Nidogen 1 (NID1)	28	18	8	10	4	6	12
22795	Nidogen 2 (NID2)	70	44	21	21	5	6	28
5118	Procollagen C-endopeptidase enhancer (PCOLCE)		1	13	5		2	5
7057	Thrombospondin 1 (THBS1)	7	3	4	4	2	2	4
7448	Vitronectin (VTN)	17	14	25	60	42	29	31
7450	Von Willebrand factor (VWF)	13	9	2	6	2	3	6
11117	Elastin microfibril interfacer 1 (EMILIN1)	44	31	115	104	102	47	74
64129	Isoform 3 of Tubulointerstitial nephritis antigen-like (TINAGL1)	8	7	5	9	2	1	5
148113	Cartilage intermediate layer protein 2 (CILP2)			13	32	9	6	15
2335	Isoform 10 of Fibronectin (FN1)	81	49	78	63	36	6	52
7045	Transforming growth factor beta induced (TGFBI)	79	37	56	75	30	36	52
7148	Tenascin XB (TNXB)	131	79	179	139	112	29	112
UniProt accession								
B4DW75	EGF-containing fibulin-like extracellular matrix protein 1 (EFEMP1)	14	8	6	9	4	2	7

Glycoproteins			
Sum of PSM means	1104	%	15

Collagens

ENTREZ GENE Accession	Protein name	P1 fresh	P1 frozen	P2 fresh	P2 frozen	P3 fresh	P3 frozen	PSM mean
1277	Collagen type I alpha 1 chain (COL1A1)	1		3	13	5		6
1278	Collagen type I alpha 2 chain (COL1A2)	2		4	6	8	4	5
1282	Collagen type IV alpha 1 chain (COL4A1)	28	13	6	37	2		17
1284	Collagen type IV alpha 2 chain (COL4A2)	22	22	11	12	11	3	14
1291	Collagen type VI alpha 1 chain (COL6A1)	462	367	573	624	318	236	430
1292	Collagen type VI alpha 2 chain (COL6A2)	196	182	244	389	186	138	223
1293	Collagen type VI alpha 3 chain (COL6A3)	1303	1217	1967	2058	1174	1094	1469
1295	Collagen type VIII alpha 1 chain (COL8A1)	4	4	4	3	1		3
1303	Collagen type XII alpha 1 chain (COL12A1)	254	245	798	735	397	241	445
7373	Collagen type XIV alpha 1 chain (COL14A1)	686	652	1309	1280	1500	740	1028
80781	Collagen type XVIII alpha 1 chain (COL18A1)	17	16	35	40	22	22	25

Collagens			
Sum of PSM means	3664	%	49

Proteoglycans

ENTREZ GENE Accession	Protein name	P1 fresh	P1 frozen	P2 fresh	P2 frozen	P3 fresh	P3 frozen	PSM mean
1634	Decorin (DCN)	8		37	27	17	4	19
2331	Fibromodulin (FMOD)	19	18	51	68	28	22	34
3339	Heparan sulfate proteoglycan 2 (HSPG2)	215	140	114	144	38	38	115
4060	Lumican (LUM)	98	73	245	224	186	108	156
4969	Osteoglycin (OGN)	155	103	311	341	168	220	216
5549	Proline and arginine rich end leucine rich repeat protein (PRELP)	2		3	6	3	2	3
127435	Podocan (PODN)	1	2	1	2	8	6	3

Proteoglycans			
Sum of PSM means	546	%	7

FIG. 3. **Ovarian matrisome proteins.** Core matrisome proteins (glycoproteins, collagens and proteoglycans) and matrisome-associated proteins (ECM-affiliated proteins, ECM regulators and secreted factors) detected with a score ≥10 in at least one sample and identified with at least 2 unique peptides in 3 or more samples were taken into consideration. The color code represents protein abundance among fresh and frozen ovarian tissues according to their PSMs. The figure explains how percentages in Fig. 4 were estimated to illustrate matrisome protein distribution in human ovarian tissue (*e.g.* glycoproteins (%) = (sum of PSM means in detected glycoproteins/total PSM mean sum of all categories)*100 = (1104/7423)*100 ≈ 15%).

Matrisom-associated proteins

ECM-affiliated proteins

ENTREZ GENE Accession	Protein name	P1 fresh	P1 frozen	P2 fresh	P2 frozen	P3 fresh	P3 frozen	PSM mean
3263	Hemopexin (HPX)	40	24	173	173	87	33	88
3956	Galectin 1 (LGALS1)	95	31	257	301	265	177	188
3958	Galectin 3 (LGALS3)	13	16	31	25	14	16	19
7123	C-type lectin domain family 3 member B (CLEC3B)	8	3	8	9	10	3	7
23654	Plexin B2 (PLXNB2)	1		4	6	2	3	3
301	Annexin A1 (ANXA1)	58	72	149	161	58	123	104
302	Annexin A2 (ANXA2)	302	250	308	440	284	483	345
307	Annexin A4 (ANXA4)	33	41	43	42	52	59	45
308	Annexin A5 (ANXA5)	200	207	459	430	385	379	343
309	Annexin A6 (ANXA6)	123	123	206	202	184	303	190
UniProt accession								
B4DT77	Annexin 7 (ANXA7)	4	6	8	15	14	13	10
B4DVE7	Annexin 11 (ANXA11)	6	15	14	18	12	17	14

ECM-affiliated proteins			
Sum of PSM means	1355	%	18

ECM regulators

ENTREZ GENE Accession	Protein name	P1 fresh	P1 frozen	P2 fresh	P2 frozen	P3 fresh	P3 frozen	PSM mean
2	Alpha-macroglobulin (A2M)	75	46	49	28	87	40	54
183	Angiotensinogen (AGT)	3	3	19	9	8	1	7
1476	Cystatin B (CSTB)	9	3	16	11	11	18	11
3273	Histidine-rich glycoprotein (HRG)	6	10	24	11	9	19	13
3697	Inter-alpha-trypsin inhibitor heavy chain 1 (ITIH1)	3	1	9	4	7	3	5
3698	Inter-alpha-trypsin inhibitor heavy chain 2 (ITIH2)	3	2	3	2	1	2	2
3700	Inter-alpha-trypsin inhibitor heavy chain family member 4 (ITIH4)	8	4	29	20	19	5	14
5265	Serpin family A member 1 (SERPINA1)	168	76	298	213	344	249	225
12	Serpin family A member 3 (SERPINA3)	8	13	30	28	5	3	15
5267	Serpin family A member 4 (SERPINA4)		2	4	2	2	1	2
1992	Serpin family B member 1 (SERPINB1)	6	1	24	15	14	13	12
5269	Serpin family B member 6 (SERPINB6)	6	5	77	59	126	43	53
462	Serpin family C member 1 (SERPINC1)	165	113	221	147	184	84	152
3053	Serpin family D member 1 (SERPIND1)	7	4	21	11	2	2	8
5270	Serpin family E member 2 (SERPINE2)	7		8	11	6	1	7
5176	Serpin family F member 1 (SERPINF1)	19	10	47	36	20	14	24
5345	Serpin family F member 2 (SERPINF2)	1	2	5	10	2		4
871	Serpin family H member 1 (SERPINH1)	33	28	28	35	33	47	34
5340	Plasminogen (PLG)	8	2	7	9	10	5	7
1508	Cathepsin B (CTSB)	5	3	3	1			3
1509	Cathepsin D (CTSD)	20	8	18	20	28	22	19
259	Alpha-1-microglobulin/bikunin precursor (AMBP)	1	4	66	22	53	27	29
UniProt accession								
B4E1H2	Plasma protease C1 inhibitor (SERPING1)	13	12	31	20	6	7	15

ECM regulators			
Sum of PSM means	715	%	10

Secreted factors

ENTREZ GENE Accession	Protein name	P1 fresh	P1 frozen	P2 fresh	P2 frozen	P3 fresh	P3 frozen	PSM mean
3054	Host cell factor C1 (HCFC1)	2		8	10	4	3	5
6277	S100 calcium binding protein A6 (S100A6)	4	1	14	12	5		7
6282	S100 calcium binding protein A11 (S100A11)	12	5	29	31	35	6	20
6284	S100 calcium binding protein A13 (S100A13)	2		5	10	11	9	7

Secreted factors			
Sum of PSM means	40	%	1

FIG. 3.—*continued*

may connect cells to elastic fibers by providing them with specific cell adhesion features (21); Fibrillin-1 has been shown to provide long-term force-bearing structural support to connective tissues and contains calcium-binding EGF-like domains, integrin-binding Arg-Gly-Asp (RGD) sequences, as well as heparin-binding domains capable of binding cell surface HSPGs (22). The presence of such structural motifs suggests that fibrillin may direct not only cell signaling, but also assembly of elastic microfibers.

Proteins related to meiosis and follicular endowment were also evaluated, namely PCNA and β-catenin as a core molecule of the WNT/β-catenin pathway and major component of cellular junctions involved in cellular communication and signal transduction. Immunohistochemical

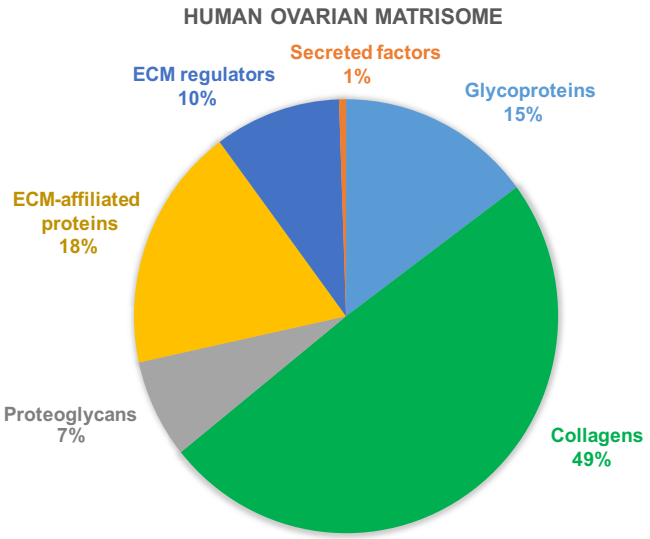

FIG. 4. **Pie chart of matrisome protein categories.**

analysis revealed PCNA-positive cells at the nuclear level in both fresh and frozen samples, as it showed positive β-catenin staining localized in the cell cytoplasm and junctions.

Because glycosaminoglycans are key components of the ECM, ensuring its homeostasis and growth factor sequestering by proteoglycans, their presence was evaluated by alcian blue staining. It revealed their diffuse distribution throughout the ovarian cortex of all patients (Fig. 7).

Western Blotting—Western blotting confirmed detection of two ECM proteoglycans; OGN and IGFALS, in the same samples analyzed by MS (Fig. 8). This is the first time that the presence of these proteins has been reported in human ovarian cortex.

Insulin-like growth factor-binding proteins such as IGFALS are known to play an important role as modulators of insulin-like growth factor (IGF) activity thanks to their high affinity (23). Indeed, they can stimulate or inhibit IGF signaling depending on circumstances by either concentrating IGF close to its receptors or, conversely, hampering sterically their binding (23). This process is of a high importance given the involvement of IGF in follicle growth regulation, selection, atresia, cellular differentiation, steroidogenesis, oocyte maturation, and cumulus expansion evidenced in animal models and humans (24–25).

Western blotting results highlighted the abundance of OGN in ovarian tissue. This protein belongs to a small leucine-rich proteoglycan (SLRP) family, a collagen-associated class of proteins that have an impact on collagen fibrillogenesis and an indirect effect on cell growth. This protein is mainly associated with bone formation and negative regulation of smooth muscle proliferation (26), but its involvement in ovarian tissue is still unknown.

DISCUSSION

The present study confidently identified 1508 proteins in fresh and frozen human ovarian cortex by 2D-LC/MS. Using bioinformatic tools and data mining analysis, we gained a deeper understanding of the function, cellular distribution and signaling role of these proteins. Although we do not yet fully discern the implication of all of them in the ovarian function, we report the most complete proteomic characterization of human ovarian cortex made to date, including a detailed description of the human ovarian ECM composition, which will lead to a better understanding of the follicle environment.

The technique described can be broadly applied to different tissues of unknown composition to provide a basic understanding of their most abundant proteins and ECM characteristics in one fraction analysis without ECM enrichment. Tissue digestion with Liberase before sample preparation for MS enabled solubilization of major fibrous proteins and thus facilitated analysis of attached molecules and characterization of the ECM. An enzymatic tissue digestion method was chosen because of the high insolubility of ECM proteins, even in strong detergents, which might hinder their detection by MS. Moreover, enzymatic digestion led to rupture of some cellular membranes, which yielded further information on intracellular proteins.

A large panel of proteins was identified within our data set, some of which had only been demonstrated *in vitro* or in animal models, but never in humans. We therefore turned to gene ontology and pathway analysis to better understand their biological role in ovarian tissue, as well as their interactions.

Fundamental cellular biological processes and several oocyte-related events were detected, namely cell communication pathways involving ECM-receptor interaction, focal adhesion and gap junctions, emphasizing the primordial functional importance of ovarian cell interaction and communication. Focal adhesion proteins made up the second largest group. Proteins included in this category were considered important for ovarian function, because focal adhesion is a key means by which cells sense and respond to the extracellular environment. Conformation of these proteins can vary in response to physical forces, and hence their function (27). This fact can be correlated with the importance of biomechanical regulation mechanisms within the ovary and the impact of the mechanical properties of scaffolds used in 3D culture on ovarian cell fate *in vitro* (28–29). Thus, greater awareness of ovarian focal adhesion proteins might provide more insights into ovarian cell communication and implication in reproduction. Gap junction channels, another detected protein category, allow direct cell-cell communication and diffusion of fundamental nutrients and chemical cues essential for follicular development (30). Their assembly is promoted by the WNT/β-catenin pathway of gap junction proteins, wherein β-catenin, a protein documented in our MS data and immu-

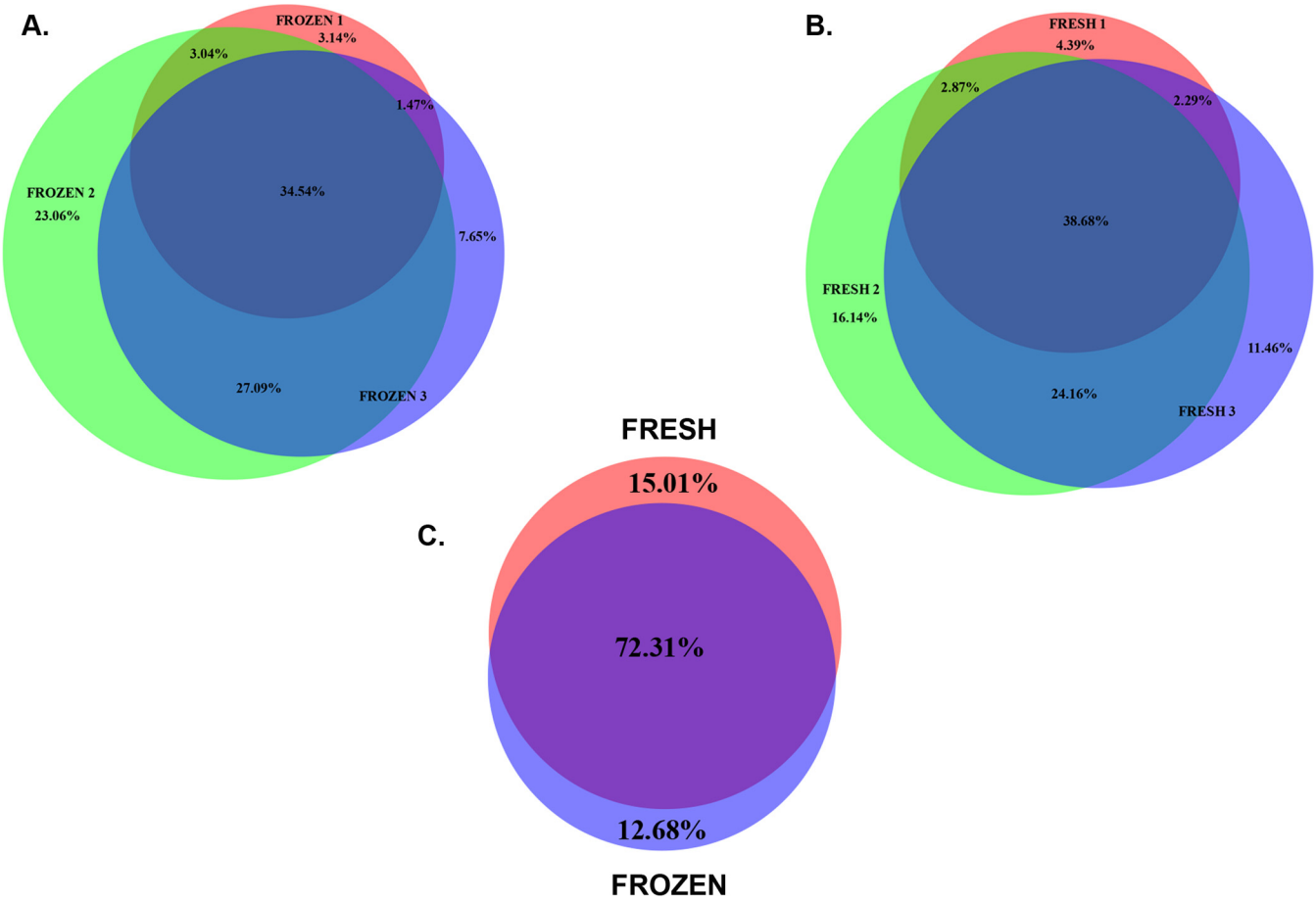

FIG. 5. **Fresh and frozen sample comparison showing the overlap of shared and unique proteins among analyzed samples from the three patients.** *A*, Overlap of fresh samples. *B*, Overlap of frozen samples. *C*, Overlap of all fresh and frozen samples. The comparison was made based on the 1508 confidently identified proteins.

nohistochemical results, plays a key role in reproduction by influencing estradiol synthesis and adversely affecting follicular development (31–32) (Fig. 7*D*).

Other pathways of interest were also detected, such as cyclic GMP-protein kinase G (cGMP/PKG) (supplemental Data S1*B*) implicated in oocyte meiotic arrest (33), and the renin-angiotensin system (RAS) that is presumed to regulate oocyte maturation and quality. Up to day, RAS involvement in hormonal regulation remains unclear because of significant differences between species (34). Hence, by means of our data set acquired by MS, we hope to contribute to the elucidation of unexplored proteins in the RAS pathway in the human ovary (supplemental Data S1*C*).

Numerous coagulation- and angiogenesis-related proteins were identified and further elucidated by KEGG pathway analysis, such as coagulation factors (*e.g.* fibrinogen, prothrombin and plasminogen), as well as those linked to the coagulation and platelet-associated regulatory system (*e.g.* antithrombin, von Willebrand factor, platelet-activating factor acetylhydrolase IB and serpins), revealing their potential function in reproduction. In 2014, Bódis *et al.* suggested the role of the platelet-associated regulatory system (PARS) in regulating activity of the hypothalamo-hypophyseal ovarian system and its function in inducing and stimulating follicular and oocyte maturation and steroid hormone secretion in the ovary (35). In the light of recent discoveries, coagulation proteins in the ovary appear to occupy new roles beyond plugging blood leakage that go as far as stem cell awakening in the ovary and ovarian rejuvenation (36–37), clearly requiring further investigation.

Although pro-angiogenic factors have been widely explored in the ovary, mainly vascular endothelial growth factor (VEGF), anti-angiogenic factors are still under-investigated. Among identified growth factors, we report detection of pigment epithelium-derived factor (PEDF), a glycoprotein known to have potent physiologic anti-angiogenic activity that negates VEGF action (38), and thus plays a potential anti-tumoral role (39). PEDF may also function as a gonadal protectant thanks to its anti-inflammatory and anti-oxidative abilities (40–41), which are two important functions in reproduction, considering that oxidative stress and inflammation have been correlated with infertility in women (38). Moreover, high levels of PEDF secreted before ovulation may induce apoptosis in ovarian sur-

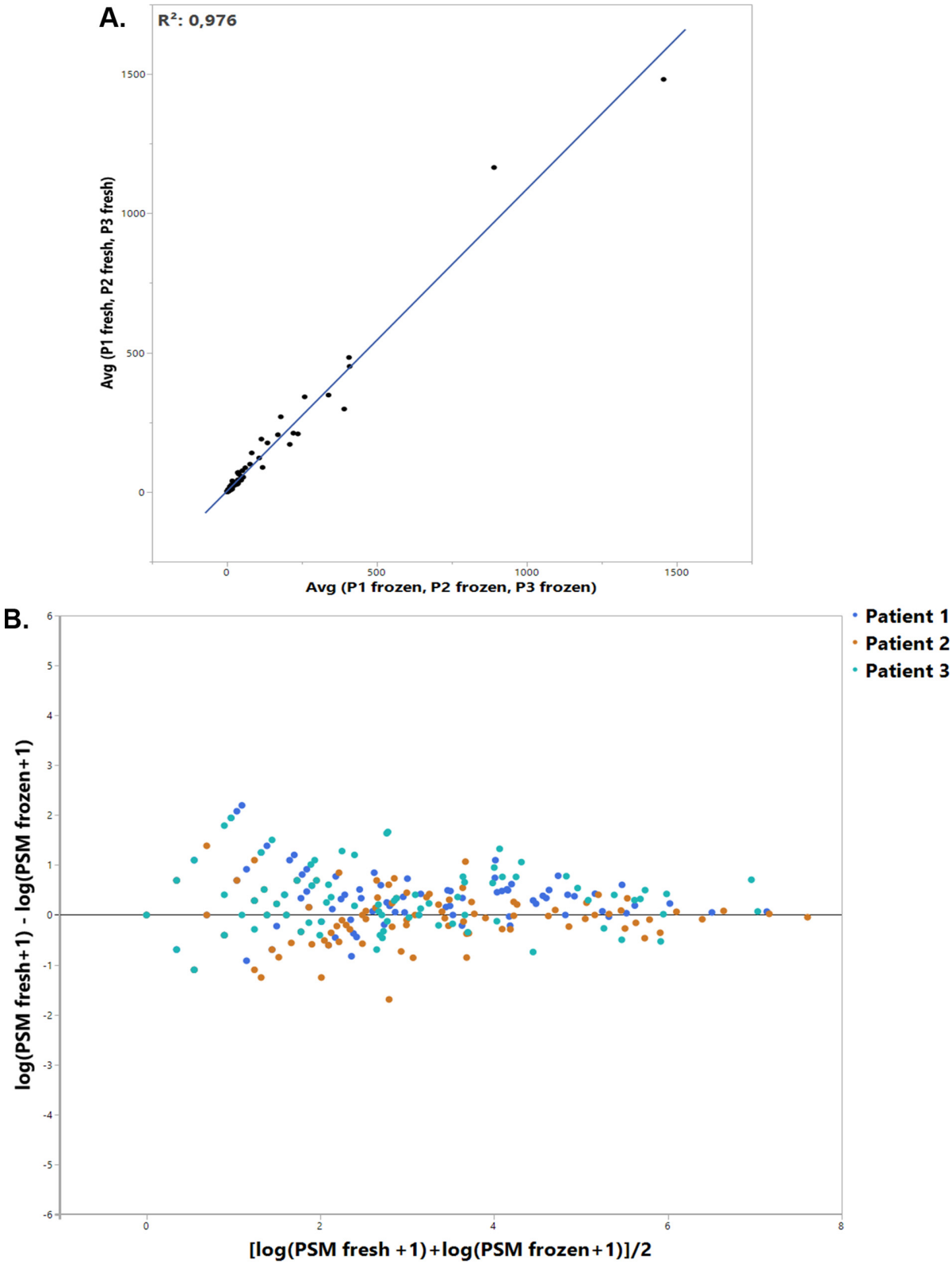

FIG. 6. **Comparison of matrisome proteins in fresh and frozen-thawed ovarian cortex samples.** *A*, Representation of the average abundance (PSMs) of each matrisome protein in both fresh and cryopreserved samples. *B*, Representation of log(PSM fresh+1) − log(PSM frozen+1) per protein in terms of log(PSM+1) mean in both samples as an abundance indicator. The extent of point deviation from the Y = 0 axis translates the difference in protein presence between fresh and frozen samples.

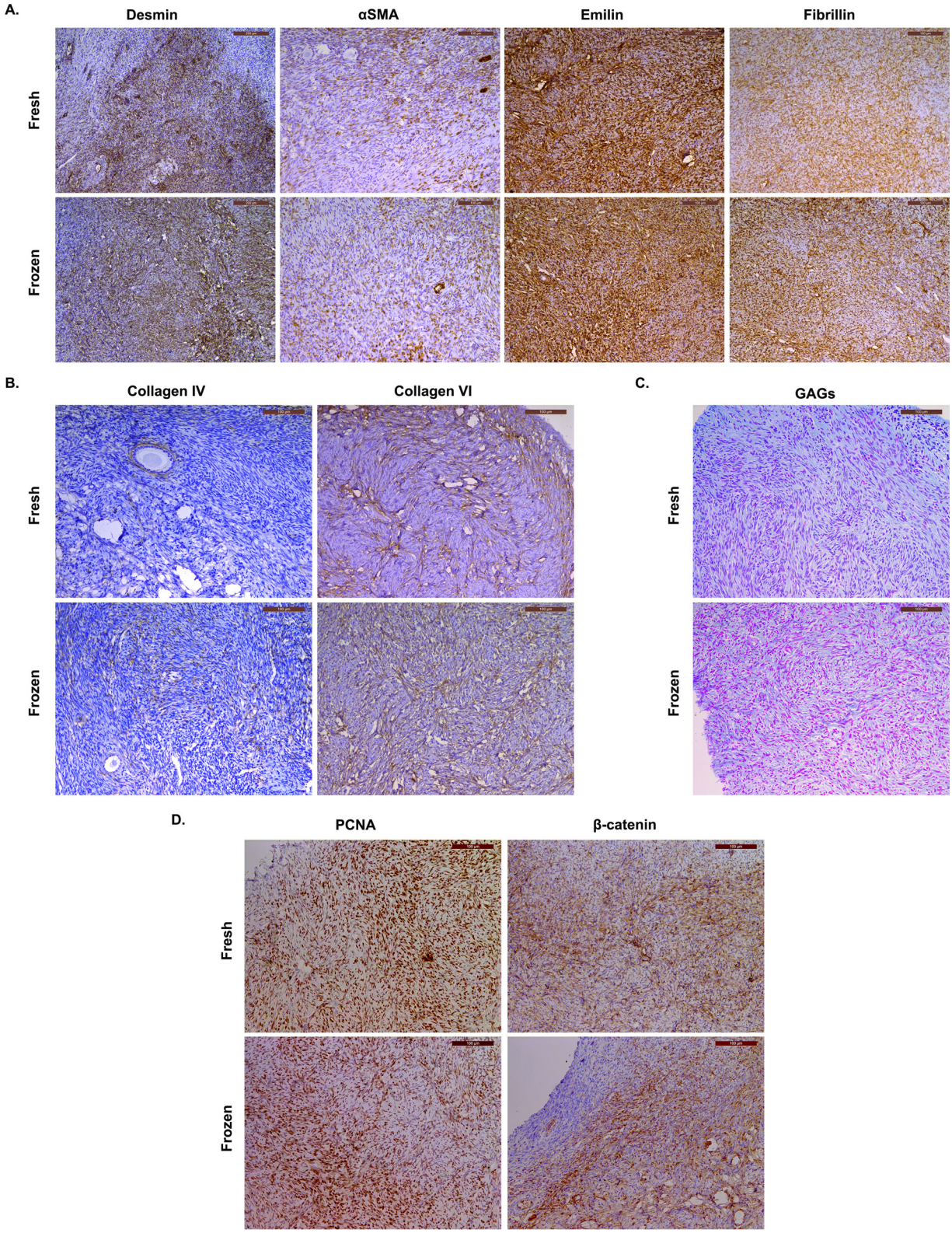

FIG. 7. **Immunohistochemical staining in fresh and cryopreserved ovarian cortex.** *A*, Desmin and αSMA were chosen as muscle contraction markers in the ovary. Emilin-1 and fibrillin-1, both ECM proteins, were selected as elasticity markers. *B*, Collagen VI, the dominant collagen type in ovarian cortex as demonstrated by MS, was analyzed to confirm proteomic results and compared with collagen IV, the most widely characterized collagen type in ovarian cortex in the literature. *C*, GAGs were stained by alcian blue at pH = 2.5 to identify carboxylated and sulfated proteoglycans. *D*, PCNA and β-catenin staining in ovarian cortex are essential proteins for meiosis and cell proliferation.

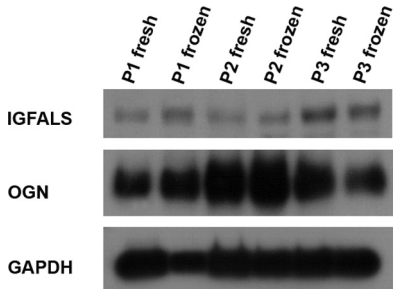

FIG. 8. **Western blotting for MS result confirmation.** Some proteins were detected for the first time in ovarian cortex during this study by MS, namely OGN and IGFALS. Western blotting was used to confirm their detection.

face epithelium cells surrounding the follicle to facilitate release of oocyte (42).

Other rarely explored proteins in human ovaries were documented in our data set, namely 14-3-3 protein isoforms delta and epsilon, which are among the top 50 most abundant proteins. 14-3-3 proteins are known to be central mediators modifying cell-signaling processes, including cell cycle regulation and apoptosis (43–46). It has been suggested that these proteins are involved, at least in the *Xenopus* genus, in maintaining prophase I arrest in germinal vesicle-intact oocytes by sequestering the key phosphatase, in meiosis resumption M-phase inducer phosphatase 2 (CDC25B), in an inactive state (47).

In view of the lack of knowledge of the follicular environment, particularly ECM proteins, this study provides the most comprehensive description available of healthy human ovarian ECM. ECM protein recognition in raw MS data was achieved by comparison of confidently detected proteins with the Matrisome Project data set (13), an *in silico* identified ECM protein set, founded on the characteristic domain-based organization of ECM proteins (48). Hence, we were able to define not only the ovarian ECM, but also the matrisome: an extended definition of the ECM and associated proteins. The dominant collagen type in the ovaries was revealed to be collagen VI, which we showed to be ubiquitously expressed throughout the ECM by immunohistochemistry. It is a basement membrane-anchoring molecule that interacts with collagen IV and may have additional cytoprotective and regulatory functions (18). In addition, it has been suggested that type VI collagen microfibrils are resistant to MMPs but are susceptible to degradation by serine proteases, which are enzymes secreted by granulocytes and neutrophils and known to be present in the ovary during the inflammatory phase preceding ovulation (49).

Within the category of glycoproteins, we identified laminin, fibrillin and thrombospondin, fundamental proteins of the basement membrane, of key importance for cellular attachment, cell proliferation and ECM organization. Most importantly, however, they share EGF-like intrinsic domains, which might bind to EGF receptors and modulate its signaling following their release by ECM proteolysis.

Within the category of proteoglycans, perlecan (HSPG2) was of interest. Like many proteoglycans, HSPG2 is able to bind growth factors and cytokines and sequester them in the ECM and may be crucially important in the action of basic fibroblast growth factor (bFGF), a key growth factor with pro-angiogenic and anti-apoptotic effects in the ovary. Localized in the basement membrane, HSPG2 provides a barrier, which is both size- and charge-selective, and promotes cell adhesion, endothelial cell growth and regeneration. In the ovary, it has been identified as a major estrogen-binding protein in follicular fluid (50).

Another proteoglycan that was unexpectedly detected is OGN, also known as osteoglycin. Its down-regulation in vascular smooth muscle cells results in an increased cell proliferation (51), which can provide insights into possible vascular stimulation of the ovarian tissue grafting site by controlling OGN expression.

In osteoblasts, bone morphogenetic protein 2 (BMP-2) increases OGN expression, whereas in the ovary, the same protein is implicated in primordial follicle assembly during fetal life (52), which might suggest the possible involvement of OGN in ovarian fetal remodeling and follicular assembly under the action of BMP-2. Further research is nevertheless needed to elucidate its function in the ovary, especially in adult life.

In the ovary, enzymatic ECM degradation is required to allow activated follicle expansion. However, to protect surrounding cells from proteolysis, different protease inhibitors appear to be secreted in the ovary, such as protein AMBP, alpha-2-macroglobulin and serpins. The latter is the most widely detected ECM regulator protein family and its expression is closely related to ovarian function (53). Indeed, folliculogenesis stage-specific expression of serpins seems to participate in the growth and atresia of follicles (54), as it may control ECM remodeling (55).

Most of ECM-affiliated proteins have seldom been studied, especially in the human ovary, where we detected galectin-1 and galectin-3. Galectins are a family of β-galactoside-binding proteins implicated in modulating cell-cell and cell-matrix interactions. In 2004, Walzel H *et al.* demonstrated the inhibitory effect of galectin-1 on the steroidogenic activity of granulosa cells, interfering with hormone-receptor interaction and resulting in decreased responses to FSH stimulation in pigs (56). Although galectin-3 has similar functions to galectin-1, it has been associated with loss of progesterone synthesis in the mouse ovary, showing increased presence in atretic preantral follicles and the later stages of luteolysis (57). This protein been described in a variety of tissues, but not explicitly in healthy human ovarian cortex. It plays a role in diverse biological events, such as embryogenesis, angiogenesis, adhesion, cellular proliferation, apoptosis and modulation of immunity and inflammatory processes (58). Overexpression of both galectins is related to ovarian carcinoma; therefore, un-

raveling the regulatory mechanisms might provide therapeutic solutions.

The third category of matrisome-associated proteins includes ECM-secreted factors. Proteins in this group were the least abundant, as expected, but several S100 proteins emerged as the most abundant protein type in this category. In fact, binding of calcium to the S100 protein causes structural rearrangement, exposing a target-binding surface. Target-binding results in a range of responses, from inflammation (S100A13) and cytoskeletal reorganization (S100A10), to cell growth control (S100A9) and tumor suppression (59–60). However, little is known about the action of these calcium-binding proteins in the ovary.

To our knowledge, this is the first time that fresh human ovarian cortex has been analyzed by MS and compared with frozen tissue cryopreserved using the protocol that has so far generated 13 live births after transplantation in our hospital. This comparison demonstrates the suitability of cryopreserved tissue to accurately represent the proteomic composition of fresh tissue, proving that it can be used to conduct more extended MS analyses.

In conclusion, our study provides an accurate first draft map of human ovarian cortex, with identification of its ECM proteins. It represents the first step in human ovary characterization, essential for development of a biomimetic artificial ovary and greater understanding of fertility in women.

Acknowledgments—We thank Olivier Van Kerk and Gaëtan Herinckx for their technical assistance, and Lieven Desmet for his advice on biostatistical evaluation. We also thank Mira Hryniuk, BA, for reviewing the English language of the manuscript.

DATA AVAILABILITY

Raw MS proteomic data were deposited in the ProteomeXchange Consortium database via the PRIDE partner repository with the data set identifier PXD008183 (https://www.ebi.ac.uk/pride/archive/projects/PXD008183).

* This study was supported by grants from the Fonds National de la Recherche Scientifique de Belgique (FNRS) (C. A. Amorim is a Research Associate, FRS - FNRS; grant M 4/1/2/5 awarded to C. A. Amorim; grant 5/4/150/5 awarded to M.-M. Dolmans).

This article contains supplemental material.

‖ To whom correspondence should be addressed: Pôle de Recherche en Gynécologie, Université Catholique de Louvain, 52 Avenue Mounier, Bte. B1.52.02, 1200 Brussels, Belgium. Tel.: +322-764-5237; E-mail: christiani.amorim@uclouvain.be.

Authors' mailing addresses: Emna Ouni: emna.ouni@uclouvain.be; Didier Vertommen: didier.vertommen@uclouvain.be; Maria Costanza Chiti: maria.chiti@uclouvain.be; Marie-Madeleine Dolmans: marie-madeleine.dolmans@uclouvain.be; Christiani A. Amorim: christiani.amorim@uclouvain.be.

REFERENCES

1. World report on disability. (2011) *Lancet,* **377,** 1977
2. Vogel, C., and Marcotte, E. M. (2012) Insights into the regulation of protein abundance from proteomic and transcriptomic analyses. *Nat. Rev. Genet.* **13,** 227–232
3. Ghaemmaghami, S., Huh, W. K., Bower, K., Howson, R. W., Belle, A., Dephoure, N., O'Shea, E. K., and Weissman, J. S. (2003) Global analysis of protein expression in yeast. *Nature* **425,** 737–741
4. Jarkovska, K., Martinkova, J., Liskova, L., Halada, P., Moos, J., Rezabek, K., Gadher, S. J., and Kovarova, H. (2010) Proteome mining of human follicular fluid reveals a crucial role of complement cascade and key biological pathways in women undergoing in vitro fertilization. *J. Proteome Res.* **9,** 1289–1301
5. Ambekar, A. S., Kelkar, D. S., Pinto, S. M., Sharma, R., Hinduja, I., Zaveri, K., Pandey, A., Prasad, T. S., Gowda, H., and Mukherjee, S. (2015) Proteomics of follicular fluid from women with polycystic ovary syndrome suggests molecular defects in follicular development. *J. Clin. Endocrinol. Metab.* **100,** 744–753
6. Angelucci, S., Ciavardelli, D., Di Giuseppe, F., Eleuterio, E., Sulpizio, M., Tiboni, G. M., Giampietro, F., Palumbo, P., and Di Ilio, C. (2006) Proteome analysis of human follicular fluid. *Biochim. Biophys. Acta.* **1764,** 1775–1785
7. He, H., Teng, H., Zhou, T., Guo, Y., Wang, G., Lin, M., Sun, Y., Si, W., Zhou, Z., Guo, X., and Huo, R. (2014) Unravelling the proteome of adult rhesus monkey ovaries. *Mol. Biosyst.* **10,** 653–662
8. Wang, L., Zhu, Y. F., Guo, X. J., Huo, R., Ma, X., Lin, M., Zhou, Z. M., and Sha, J. H. (2005) A two-dimensional electrophoresis reference map of human ovary. *J. Mol. Med.* **83,** 812–821
9. Heeren, A. M., van Iperen, L., Klootwijk, D. B., de Melo Bernardo, A., Roost, M. S., Gomes Fernandes, M. M., Louwe, L. A., Hilders, C. G., Helmerhorst, F. M., van der Westerlaken, L. A., Chuva de Sousa Lopes, S. M. (2015) Development of the follicular basement membrane during human gametogenesis and early folliculogenesis. *BMC Dev. Biol.* **15**, 4
10. Rodgers, R. J., Irving-Rodgers, H. F., and Russell, D. L. (2003) Extracellular matrix of the developing ovarian follicle. *Reproduction* **126,** 415–424
11. Vanacker, J., Camboni, A., Dath, C., Van Langendonckt, A., Dolmans, M. M., Donnez, J., Amorim, C. A., (2011) Enzymatic isolation of human primordial and primary ovarian follicles with Liberase DH: protocol for application in a clinical setting. *Fertil. Steril.* **96,** 379–383.e3
12. Amorim, C. A., Van Langendonckt, A., David, A., Dolmans, M. M., and Donnez, J. (2009) Survival of human pre-antral follicles after cryopreservation of ovarian tissue, follicular isolation and in vitro culture in a calcium alginate matrix. *Hum. Reprod.* **24,** 92–99
13. Naba, A., Clauser, K. R., Ding, H., Whittaker, C. A., Carr, S. A., and Hynes, R. O. (2016) The extracellular matrix: Tools and insights for the "omics" era. *Matrix Biol* **49,** 10–24
14. Quintarelli, G., and Dellovo, M. C. (1965) The chemical and histochemical properties of alcian blue. IV. Further studies on the methods for the identification of acid glycosaminoglycans. *Histochemie* **5,** 196–209
15. Smith, R. M., Woodruff, T. K., and Shea, L. D. (2010) Designing follicle-environment interactions with biomaterials. *Cancer Treat. Res.* **156,** 11–24
16. Woodruff, T. K., and Shea, L. D. (2007) The role of the extracellular matrix in ovarian follicle development. *Reprod. Sci.* **14,** 6–10
17. Irving-Rodgers, H. F., and Rodgers, R. J. (2005) Extracellular matrix in ovarian follicular development and disease. *Cell Tissue Res.* **322,** 89–98
18. Cescon, M., Gattazzo, F., Chen, P., Bonaldo, P., and Collagen, V. I. (2015) at a glance. *J. Cell Sci.* **128,** 3525–3531
19. Zhang, H., Apfelroth, S. D., Hu, W., Davis, E. C., Sanguineti, C., Bonadio, J., Mecham, R. P., and Ramirez, F. (1994) Structure and expression of fibrillin-2, a novel microfibrillar component preferentially located in elastic matrices. *J. Cell Biol.* **124,** 855–863
20. The UniProt Consortium. (2017) UniProt: the universal protein knowledgebase. *Nucleic Acids Res.* **45,** D158–D169
21. Danussi, C., Petrucco, A., Wassermann, B., Pivetta, E., Modica, T. M., Del Bel. (2011) Belluz, L., Colombatti, A., Spessotto, P., EMILIN1-alpha4/alpha9 integrin interaction inhibits dermal fibroblast and keratinocyte proliferation. *J. Cell Biol.* **195,** 131–145
22. Theocharis, A. D., Skandalis, S. S., Gialeli, C., and Karamanos, N. K. (2016) Extracellular matrix structure. *Adv. Drug Deliv. Rev.* **97,** 4–27
23. Bach, L. A. (2015) Insulin-like growth factor binding proteins 4–6. *Best Pract. Res. Clin. Endocrinol. Metab.* **29,** 713–722
24. Sirotkin, A. V. (2011) Growth factors controlling ovarian functions. *J. Cell. Physiol.* **226,** 2222–2225
25. Wandji, S. A., Gadsby, J. E., Simmen, F. A., Barber, J. A., and Hammond, J. M. (2000) Porcine ovarian cells express messenger ribonucleic acids for the acid-labile subunit and insulin-like growth factor binding protein-3

during follicular and luteal phases of the estrous cycle. *Endocrinology* **141,** 2638–2647
26. Funderburgh, J. L., Funderburgh, M. L., Mann, M. M., Corpuz, L., and Roth, M. R. (2001) Proteoglycan expression during transforming growth factor beta -induced keratocyte-myofibroblast transdifferentiation. *J. Biol. Chem.* **276,** 44173–44178
27. Wu, C. (2007) Focal adhesion: a focal point in current cell biology and molecular medicine. *Cell Adh. Migr.* **1,** 13–18
28. Wood, C. D., Vijayvergia, M., Miller, F. H., Carroll, T., Fasanati, C., Shea, L. D., Brinson, L. C., and Woodruff, T. K. (2015) Multi-modal magnetic resonance elastography for noninvasive assessment of ovarian tissue rigidity in vivo. *Acta Biomater.* **13,** 295–300
29. West, E. R., Xu, M., Woodruff, T. K., and Shea, L. D. (2007) Physical properties of alginate hydrogels and their effects on in vitro follicle development. *Biomaterials* **28,** 4439–4448
30. McGinnis, L. K., and Kinsey, W. H. (2015) Role of focal adhesion kinase in oocyte-follicle communication. *Mol. Reprod. Dev.* **82,** 90–102
31. DaganWells, Z. H. a., Molecular aspects of follicular development. In *Principles and Practice of Fertility Preservation*, Cambridge University Press: Cambridge, 2011; pp 114–128
32. Parakh, T. N., Hernandez, J. A., Grammer, J. C., Weck, J., Hunzicker-Dunn, M., Zeleznik, A. J., and Nilson, J. H. (2006) Follicle-stimulating hormone/cAMP regulation of aromatase gene expression requires beta-catenin. *Proc. Natl. Acad. Sci. U.S.A.* **103,** 12435–12440
33. Vaccari, S., and Weeks, J. L. (2009) 2nd; Hsieh, M., Menniti, F. S., Conti, M., Cyclic GMP signaling is involved in the luteinizing hormone-dependent meiotic maturation of mouse oocytes. *Biol. Reprod.* **81,** 595–604
34. Herr, D., Bekes, I., Wulff, C. (2013) Local Renin-Angiotensin system in the reproductive system. *Front. Endocrinol.* **4**, 150
35. Bodis, J., Papp, S., Vermes, I., Sulyok, E., Tamas, P., Farkas, B., Zambo, K., Hatzipetros, I., and Kovacs, G. L., (2007) "Platelet-associated regulatory system (PARS)" with particular reference to female reproduction. *J. Ovarian Res.* **7,** 55
36. Bukovsky, A. (2015) Novel methods of treating ovarian infertility in older and POF women, testicular infertility, and other human functional diseases. *Reprod. Bio.l Endocrinol.* **13,** 10
37. Hirota, Y., Osuga, Y., Yoshino, O., Koga, K., Yano, T., Hirata, T., Nose, E., Ayabe, T., Namba, A., Tsutsumi, O., and Taketani, Y. (2003) Possible roles of thrombin-induced activation of protease-activated receptor 1 in human luteinized granulosa cells. *J. Clin. Endocrinol. Metab.* **88,** 3952–3957
38. Chuderland, D., Ben-Ami, I., Bar-Joseph, H., and Shalgi, R. (2014) Role of pigment epithelium-derived factor in the reproductive system. *Reproduction* **148,** R53–R61
39. Cheung, L. W., Au, S. C., Cheung, A. N., Ngan, H. Y., Tombran-Tink, J., Auersperg, N., and Wong, A. S. (2006) Pigment epithelium-derived factor is estrogen sensitive and inhibits the growth of human ovarian cancer and ovarian surface epithelial cells. *Endocrinology* **147,** 4179–4191
40. Yamagishi, S., Nakamura, K., Ueda, S., Kato, S., and Imaizumi, T. (2005) Pigment epithelium-derived factor (PEDF) blocks angiotensin II signaling in endothelial cells via suppression of NADPH oxidase: a novel anti-oxidative mechanism of PEDF. *Cell Tissue Res.* **320,** 437–445
41. Wang, J. J., Zhang, S. X., Mott, R., Chen, Y., Knapp, R. R., Cao, W., and Ma, J. X. (2008) Anti-inflammatory effects of pigment epithelium-derived factor in diabetic nephropathy. *Am. J. Physiol. Renal Physiol.* **294,** F1166–F1173
42. Auersperg, N., Wong, A. S., Choi, K. C., Kang, S. K., and Leung, P. C. (2001) Ovarian surface epithelium: biology, endocrinology, and pathology. *Endocr. Rev.* **22,** 255–288
43. Pozuelo Rubio, M., Geraghty, K. M., Wong, B. H., Wood, N. T., Campbell, D. G., Morrice, N., and Mackintosh, C. (2004) 14-3-3-affinity purification of over 200 human phosphoproteins reveals new links to regulation of cellular metabolism, proliferation and trafficking. *Biochem. J.* **379,** 395–408
44. Aitken, A. (2006) 14-3-3 proteins: a historic overview. *Semin. Cancer Biol.* **16,** 162–172
45. Morrison, D. K. (2009) The 14-3-3 proteins: integrators of diverse signaling cues that impact cell fate and cancer development. *Trends Cell Biol.* **19,** 16–23
46. Freeman, A. K., and Morrison, D. K. (2011) 14-3-3 Proteins: diverse functions in cell proliferation and cancer progression. *Semin. Cell Dev. Biol.* **22,** 681–687
47. Duckworth, B. C., Weaver, J. S., and Ruderman, J. V. (2002) G2 arrest in Xenopus oocytes depends on phosphorylation of cdc25 by protein kinase A. *Proc. Natl. Acad. Sci. U.S.A.* **99,** 16794–16799
48. Naba, A., Clauser, K. R., Hoersch, S., Liu, H., Carr, S. A., Hynes, R. O. (2012) The matrisome: in silico definition and in vivo characterization by proteomics of normal and tumor extracellular matrices. *Mol. Cell. Proteomics* **11,** M111.014647
49. Iwahashi, M., Muragaki, Y., Ooshima, A., Nakano, R., and Type, V. I. (2000) collagen expression during growth of human ovarian follicles. *Fertil. Steril.* **74,** 343–347
50. Bentov, Y., Jurisicova, A., Kenigsberg, S., and Casper, R. F. (2016) What maintains the high intra-follicular estradiol concentration in pre-ovulatory follicles? *J. Assist. Reprod. Genet.* **33,** 85–94
51. Deckx, S., Heggermont, W., Carai, P., Rienks, M., Dresselaers, T., Himmelreich, U., van Leeuwen, R., Lommen, W., van der Velden, J., Gonzalez, A., Diez, J., Papageorgiou, A. P., and Heymans, S. (2017) Osteoglycin prevents the development of age-related diastolic dysfunction during pressure overload by reducing cardiac fibrosis and inflammation. *Matrix Biol.* **66,** 110–124
52. Chakraborty, P., and Roy, S. K. (2015) Bone morphogenetic protein 2 promotes primordial follicle formation in the ovary. *Sci. Rep.* **5,** 12664
53. Ny, T., Wahlberg, P., and Brandstrom, I. J. (2002) Matrix remodeling in the ovary: regulation and functional role of the plasminogen activator and matrix metalloproteinase systems. *Mol. Cell. Endocrinol.* **187,** 29–38
54. Hayashi, K. G., Ushizawa, K., Hosoe, M., and Takahashi, T. (2011) Differential gene expression of serine protease inhibitors in bovine ovarian follicle: possible involvement in follicular growth and atresia. *Reprod. Biol. Endocrinol.* **9,** 72
55. Law, R. H., Zhang, Q., McGowan, S., Buckle, A. M., Silverman, G. A., Wong, W., Rosado, C. J., Langendorf, C. G., Pike, R. N., Bird, P. I., and Whisstock, J. C. (2006) An overview of the serpin superfamily. *Genome Biol* **7,** 216
56. Walzel, H., Brock, J., Pohland, R., Vanselow, J., Tomek, W., Schneider, F., and Tiemann, U. (2004) Effects of galectin-1 on regulation of progesterone production in granulosa cells from pig ovaries in vitro. *Glycobiology* **14,** 871–881
57. Nio, J., and Iwanaga, T. (2007) Galectins in the mouse ovary: concomitant expression of galectin-3 and progesterone degradation enzyme (20alpha-HSD) in the corpus luteum. *J Histochem Cytochem* **55,** 423–432
58. Devouassoux-Shisheboran, M., Deschildre, C., Mauduit, C., Berger, G., Mejean-Lebreton, F., Bouvier, R., Droz, J. P., Fenichel, P., and Benahmed, M. (2006) Expression of galectin-3 in gonads and gonadal sex cord stromal and germ cell tumors. *Oncol. Rep.* **16,** 335–340
59. Donato, R. (2001) S100: a multigenic family of calcium-modulated proteins of the EF-hand type with intracellular and extracellular functional roles. *Int. J. Biochem. Cell Biol.* **33,** 637–668
60. Santamaria-Kisiel, L., Rintala-Dempsey, A. C., and Shaw, G. S. (2006) Calcium-dependent and -independent interactions of the S100 protein family. *Biochem. J.* **396,** 201–214